A marked interannual variability of haze linked to particulate sources and meteorological conditions in Tehran (Iran), 1990-2020

Zahra Pashaie[1,*], Behrooz Sari Sarraf[1], Cesar Azorin-Molina[2], Gholam Hassan Mohammadi[3], Jose A. Guijarro[4]

1. Climatology Department, Faculty of Planning and Environmental Sciences, University of Tabriz, Tabriz, Iran

2. Centro de Investigaciones sobre Desertificación, Consejo Superior de Investigaciones Científicas (CIDE, CSIC-UV-*Generalitat Valenciana*), Climate, Atmosphere and Ocean Laboratory (Climatoc-Lab), Moncada, Valencia, Spain

3. I.R. of Iran Meteorological Organization, East Azerbaijan Province Central Bureau of Meteorology, Tabriz, Iran

4. Retired from the State Meteorological Agency (AEMET), Balearic Islands Office, Palma de Mallorca, Spain

* *Corresponding author address*: Zahra Pashaie, Climatology Department, Faculty of Planning and Environmental Sciences, University of Tabriz, 29 Bahman Blvd, Tabriz 51664, Iran

E-mail: z.pashaie@tabrizu.ac.ir

Manuscript submitted to *Urban Climate*

December 2022

A marked interannual variability of haze linked to particulate sources and meteorological conditions in Tehran (Iran), 1990-2020

Zahra Pashaie[1,*], Behrooz Sari Sarraf[1], Cesar Azorin-Molina[2], Gholam Hassan Mohammadi[3], Jose A. Guijarro[4]

1. Climatology Department, Faculty of Planning and Environmental Sciences, University of Tabriz, Tabriz, Iran

2. Centro de Investigaciones sobre Desertificación, Consejo Superior de Investigaciones Científicas (CIDE, CSIC-UV-*Generalitat Valenciana*), Climate, Atmosphere and Ocean Laboratory (Climatoc-Lab), Moncada, Valencia, Spain

3. I.R. of Iran Meteorological Organization, East Azerbaijan Province Central Bureau of Meteorology, Tabriz, Iran

4. Retired from the State Meteorological Agency (AEMET), Balearic Islands Office, Palma de Mallorca, Spain

* *Corresponding author address*: Zahra Pashaie, Climatology Department, Faculty of Planning and Environmental Sciences, University of Tabriz, 29 Bahman Blvd, Tabriz 51664, Iran

E-mail: z.pashaie@tabrizu.ac.ir

Manuscript submitted to *Urban Climate*

December 2022

ABSTRACT

This research assessed for the first time the spatio-temporal changes of haze pollution (NHAZEs) and its relationship with levels of gaseous pollutants and meteorological conditions over Tehran metropolis (Iran) for 1990-2020. The results showed a significant decreasing trend of NHAZEs annually and in winter, along with a significant increasing trend in the horizontal visibility. However, a marked interannual variability linked to changes in $PM_{2.5}$ concentrations and the influence of meteorological conditions was detected, which explained 65% and 30% of the NHAZEs variances, respectively. We found that the increasing trend of wind speed annually and in winter is the principal driver behind the decrease in NHAZEs and the increase in visibility; as winds control the movement and dispersion of air pollution. In relation to gaseous pollutants, a case study showed that the highest concentrations of $PM_{2.5}$ and NHAZEs were recorded under high levels of SO2, CO, and NO2, and low levels of O3, which mainly occurred under stable anticyclonic circulations. Spatially, the NHAZEs mostly affected the western, southwestern, central, and some parts of the northern of Tehran metropolis, because of the location of industries, traffic, and lack of green areas.

KEY WORDS: Haze, visibility, trends, $PM_{2.5}$, meteorological influence, Tehran metropolis

1. Introduction

Haze is a common synoptic phenomenon (World Meteorological Organization, 2019) primarily caused by $PM_{2.5}$, in which visibility is less than 10 km, and relative humidity (RH) values below 90% (Yang et al., 2016; Shi et al., 2019). The cause of atmospheric turbidity when RH is less than 90% is the occurrence of haze as other meteorological phenomena such as rain, snow and hail, which are atmospheric turbidity factors, usually occur when RH is higher than 90%. Haze events are frequently related to particulate air pollution and low atmospheric visibility (Ding et al., 2009; Hyslop, 2009; He et al., 2018; An et al., 2019; Wei et al., 2020). Therefore, it causes harmful effects such as increased deaths from cardiovascular and respiratory diseases (Kampa and Castanas, 2008; Xingqin et al., 2015; Cohen et al., 2017; Liu et al., 2019), and reduced safety of road, air, and rail transport (Wang et al. 2020), to name but a few. In recent years, the study of haze has attracted the scientific interest due to its harmful effects on human health and economic development, and many scientists around the world have studied various aspects of it, including the characteristics and formation mechanisms (Li et al., 2017; Ye et al., 2019; He et al., 2021; Van et al., 2022), the role of anthropogenic emissions (Yang et al., 2016; Liu et al., 2022), the influence of meteorological conditions (Yang et al., 2016; He et al., 2018; Shi et al., 2019; Yin et al., 2021), and the impact on climate change and the effects of teleconnections (Shen et al., 2018; Zhao et al., 2018; Wang et al., 2020; Yin et al., 2020; Zhao et al., 2022), among others. These studies are mainly concerned about haze pollution in metropolises, with results that highly depend on the features of the study area, large-scale atmospheric circulation and climate drivers such as teleconnection patterns, and the proximity to pollutant emission sources. Therefore, site-specific studies to determine the spatio-temporal variability of haze in e.g. highly polluted industrial cities such as Tehran (Iran), is strongly needed.

Tehran occupies a central political and economic role as Iran's capital which is one of the largest and most populous cities in the world. Tehran is located between 35.35º to 35.48º N latitude and 51.17º to 51.33º E longitude, at a high altitude (1,200 m a.s.l.), and is surrounded by the Alborz Mountain Range which strongly affects the dispersion pattern of pollutants (Safavi and Alijani, 2006; Ashrafi, 2012); Figure 1. The city has an area of about 730 km^2 with a population of 8 million (Statistical Center of Iran, 2022). According to the Köppen-Geiger climate classification, Tehran has a semi-arid climate (Raziei, 2017) and is a little cooler than other Middle Eastern capitals due to its higher latitude and altitude. The air in Tehran is amongst the most polluted in the world (World Bank staff based on data from WHO, 2016). Air pollution is a major problem in Tehran (Shahbazi et al., 2016). Urbanization, rapid population growth, increasing fuel consumption, and industrial development are pressure points for clean air in Tehran (Heger and Sarraf, 2018). Tehran is one of the most polluted cities, and various studies have analyzed its pollution due to the need of establishing regional pollution control strategies. According to the findings of these studies, the natural conditions of the Tehran metropolis have a high impact on the dispersion pattern of pollutants; e.g., local wind circulations are very effective in the dispersion of air pollution (Safavi and Alijani, 2006; Ramezani et al., 2018; Pishdad et al., 2020). Studies have shown an increase in $PM_{2.5}$ in recent years in Tehran (Torbatian et al., 2019). Most of the studies have examined Tehran's pollution using qualitative air index data during short-term periods (Hejazizadeh et al., 2017; Yasar et al., 2020; Ali-Taleshi et al., 2022). But to the best of our knowledge, there has been no research examining the multidecadal spatio-temporal changes of haze pollution in Tehran. In view of this research gap, the overall aim of this study is to assess for the first time the long-term changes and spatio-temporal variability of winter haze in Tehran for a 31-yr 1990-2020 study period. Here we also analyze the relationship with levels of gaseous pollutants and meteorological conditions.

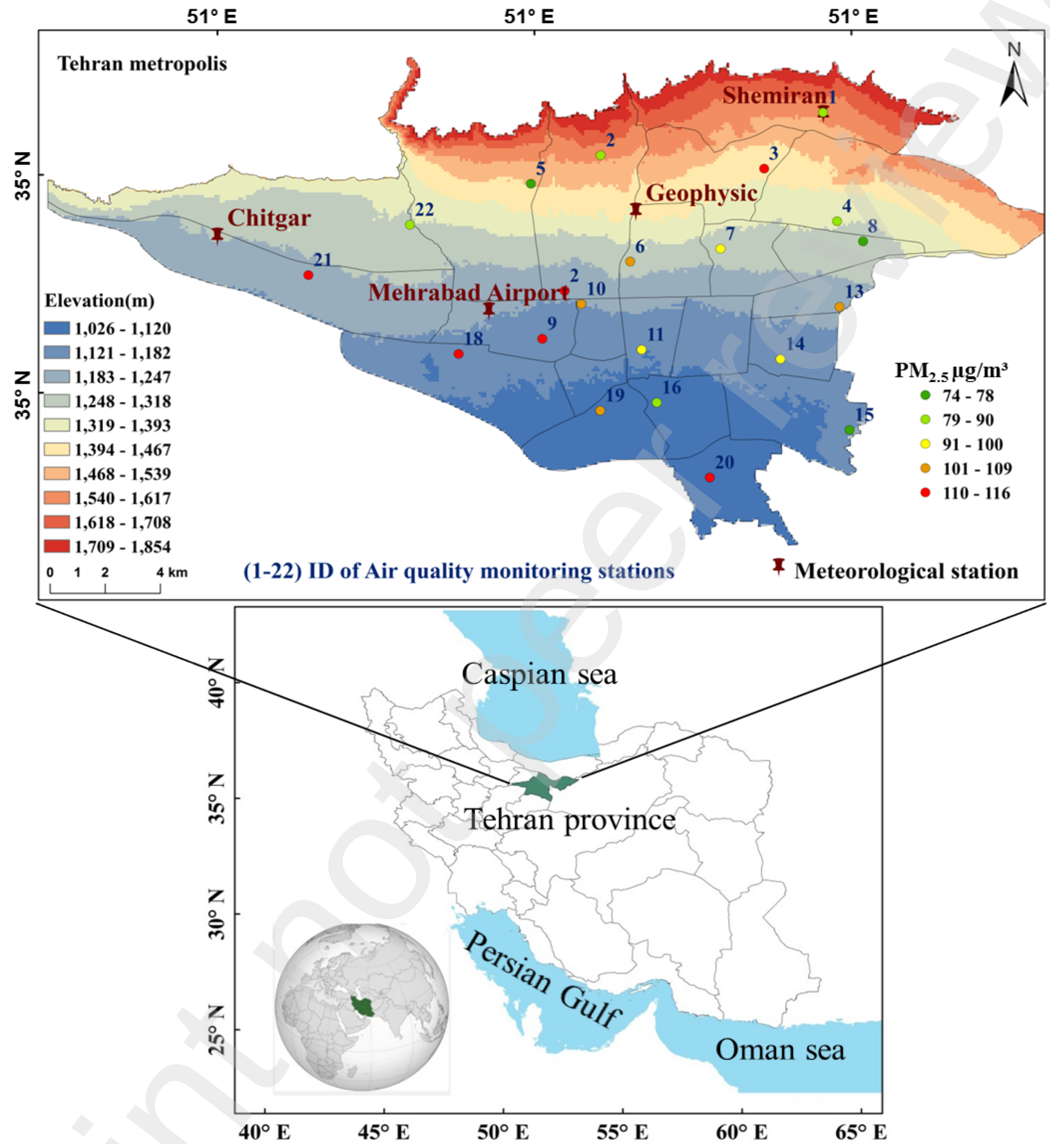

Figure 1: Elevation map of Tehran region with location of the meteorological stations and the average of $PM_{2.5}$ in the monitoring stations used in this study. Details for the air quality monitoring stations are given in Table 1.

2. Data and methods

2.1. The number of haze synop (NHAZEs)

Visibility, RH, and suspended particles are three attributes of haze (He et al., 2018), which cause this phenomenon when visibility is less than 10 km and RH is less than 90% (Ding et al., 2014). Specific codes are used in meteorological stations to express the current weather. During the Coordinated Universal Time (UTC), these codes are sent to the Iran Meteorological Organization (IRIMO, https://data.irimo.ir/; last accessed 27 November 2022). Code 05 is used to record the haze phenomenon which occurs under the abovementioned conditions. Data for the current weather code on the Synop scale (every 3 hours) for the stations analyzed in this study were taken from the IRIMO. Haze events generally occur during the winter because of occurrence of air temperature inversions. Air usually cools with altitude, but warm air settles above a layer of cool air near the surface during an inversion. The warm air acts like a lid and traps pollutants near the surface, especially in basins and valleys. Due to the maximum occurrence of haze in Tehran in winter, we particularly focused on winter haze as also conducted previous studies (Xiao et al., 2015; Shi et al., 2019; Zhao et al., 2020; Li et al., 2021; Zhang et al., 2021). Since some stations do not report meteorological codes at night, we removed the data recorded at 06:00 PM, 09:00 PM, 12:00 AM, and 03:00 AM local time. Then, the haze synop (reported with code 05) was counted in the annual and seasonal (winter) scales for the 31-year 1990-2020 study period, and the frequency (in synops) of haze was calculated. Boreal winter season is defined as December, January and February.

2.2. Observed air quality data

According to studies conducted around the world, haze is mainly caused by aerosol pollution (Li et al., 2017; Gan et al., 2020; He et al., 2021). To explore the relationship between the variability of haze and suspended particles, we received data on air pollutants from the Tehran Air Quality Control Company (for locations see Fig 1. and details in Table 1). However, there is no long-term observation series of $PM_{2.5}$ (in µg/m3) as the primary cause of haze (Li et al., 2017; Ye et al., 2019) in Tehran because the $PM_{2.5}$ concentrations have been observed and released since 2009 in Iran (only in a few stations). Since 2013, $PM_{2.5}$ concentrations have been recorded in all stations. The data is available for downloading at https://air.tehran.ir/ (last accessed 15 October 2022).

Table 1: Specifications of air quality monitoring stations used in Tehran. For locations see ID in Figure 1.

ID	Station name	Latitude (decimal degree)	Longitude (decimal degree)	Elevation (m a.s.l.)	Start year
1	Agdasiyeh	35.80	51.48	1,562	2000
2	Sharif	35.70	51.34	1,188	2012
2	Region 2	35.77	51.36	1,562	2012
3	Dorus	35.77	51.45	1,415	2010
4	Region 4	35.74	51.49	1,337	2009
5	Punak	35.76	51.33	1,467	2007
6	Tarbiat Modarres	35.72	51.38	1,287	2012
7	Setadbohran	35.67	51.30	1,162	2011
8	Golbarg	35.73	51.50	1,287	2008
9	Fath	35.67	51.33	1,137	2010
10	Region 10	35.69	51.35	1,137	2009
11	Region 11	35.67	51.38	1,137	2009
13	Piruzi	35.70	51.50	1,214	2011
14	Mahallati	35.66	51.46	1,137	2010
15	Masoudieh	35.63	51.50	1,162	2013
16	Region 16	35.64	51.40	1,093	2009
18	Shadabad	35.67	51.30	1,162	2011
19	Region 19	35.64	51.36	1,093	2009
21	Shahrrey	35.60	51.42	1,043	2005
22	Park roz	35.74	51.26	1,311	2017

2.3. Observed and reanalyzed meteorological data

Observed data from 4 synoptic meteorological stations in Tehran (for location names see Fig 1. and details in Table 2), including three hour air temperature (T in ºC), relative humidity (RH in %), visibility (VIS, in m), wind speed (WS, in m s^{-1}), wind direction (WD, in º), and sea level pressure (SLP in hPa) from 1990 to 2020 were obtained from IRIMO (https://data.irimo.ir/; last accessed 27 November 2022). Furthermore, the European Centre for Medium-Range Weather Forecasts (ECMWF) ERA5 reanalysis data (https://cds.climate.copernicus.eu/cdsapp/dataset/reanalysis-era5-land; last accessed 27 November 2022) for the 31 year period (1990-2020) were also used to apply a robust quality control and homogenization protocol of the meteorological data (for details see section 2.4). ERA5 is the fifth generation ECMWF atmospheric reanalysis of the global climate covering the period from January 1950 to the present. The horizontal resolution of ECMWF ERA5 data is 0.1° x 0.1°, and the temporal resolution is hourly.

Table2: Specifications of the meteorological stations used in Tehran. For locations, see Fig. 1.

	Station ID	Station name	Latitude (decimal degree)	Longitude (decimal degree)	Elevation (m a.s.l.)	Time period
1	99331	Tehran (Geophysic)	35.74	51.38	1,418	1991-2020
2	40751	Tehran (Shemiran)	35.79	51.48	1,549	1988-2020
3	40754	Tehran (Mehrabad Airport)	35.69	51.30	1,191	1951-2020
4	99320	Chitgar	35.73	51.16	1,305	1996-2020

2.4. Homogenization of observed meteorological data

The homogenization method implemented in the R package CLIMATOL was used to homogenize the meteorological data. This robust protocol detects sudden breakpoints using the well-established relative Standard Normal Homogeneity Test (SNHT) (Alexandersson, 1986), which has effectively been used in previous homogenization research (Azorin-Molina et al., 2014, 2017; to name but a few). The R Climatol homogenization package (Guijarro, 2018) performs its process in three main stages, with much iteration within them. The first two are devoted to removing unwanted outliers and splitting the series found most inhomogeneous into two fragments at the term where the SNHT was more significant. Successive iterations refine the process until no outlier nor are shift detected over preset thresholds. In the first stage, SNHT is applied on stepped overlapping windows along with the series to diminish possible masking problems when several shifts are present, while in the second stage, SNHT is applied over the whole series, getting all the power of the test. These outlier rejections and shift detection are performed over a series of differences (anomalies) between the observed data and a synthetic reference series built from a number of nearby grid-points in ERA-5, in both cases in normalized form. Normalization can be chosen within full standardization (the default), ratio to the mean, or difference to the mean. The last third stage is dedicated to assigning their synthetic values to all the missing data in all the series and sub-series that originated in the splitting process. The number of detected and corrected break-points was 28 in the VIS data series, 17 in the WS data series, 16 in the RH data series, and 9 in the T data series. WD data series did not pass any homogenization protocol due to its complexity and were only used for analyzing a study case. After completing the robust quality control and homogenization protocol, 4 homogeneous meteorological series were used for 1990-2020.

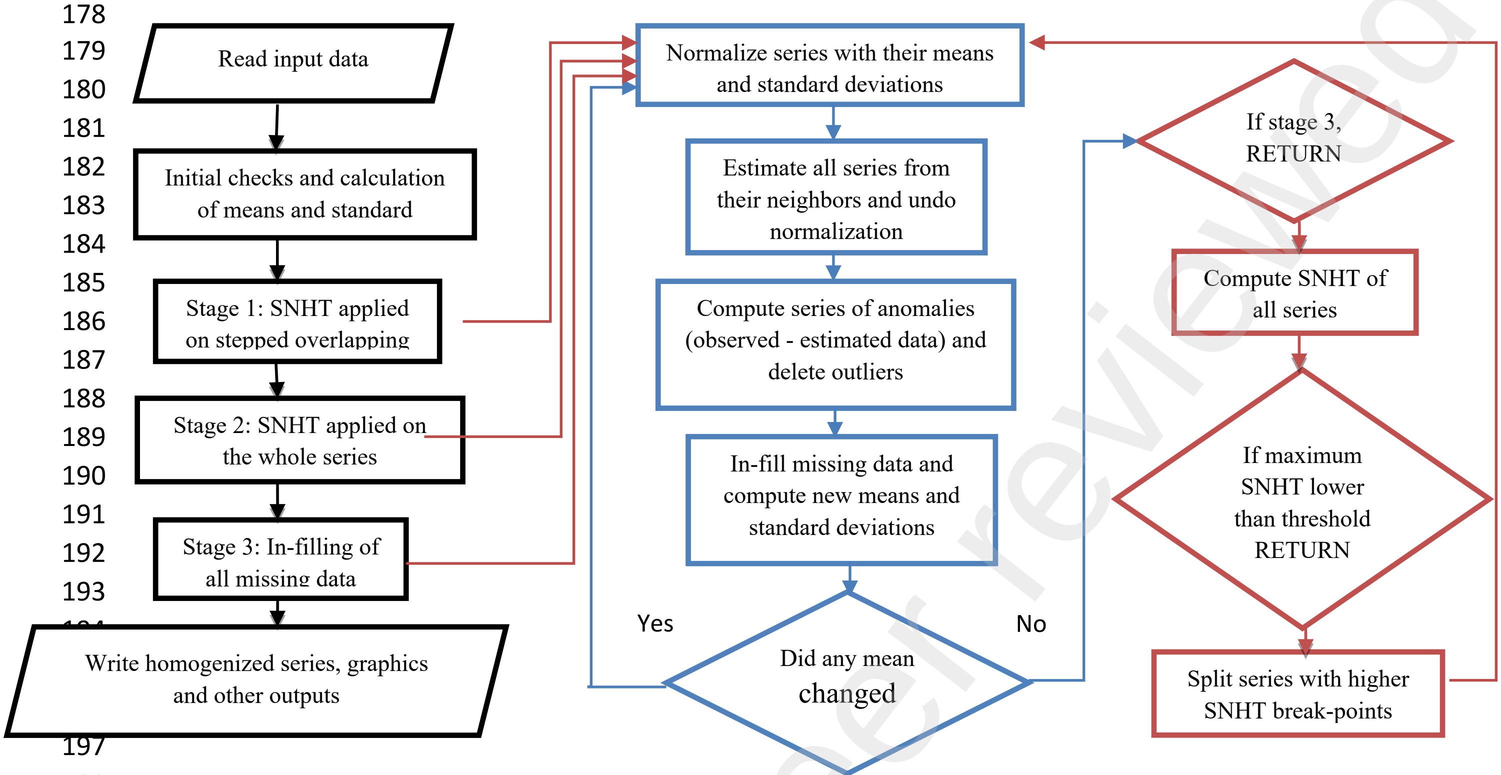

Figure 2: Flow-chart of the Climatol protocol to quality control and homogenize meteorological data, showing its nested iterative processes. SNHT is the abbreviation for the Standard Normal Homogeneity Test.

2.5. Trend analysis and statistics

Sen's Slope Estimator test is recommended by the World Meteorological Organization as part of the trend detection in hydrometeorological data (WMO, 2019). The trend is supposed to be linear in this test and indicates the quantification of temporal change (Aditya et al., 2021). The Sen's Slope equation for a number of N data sample pairs is written as follows (Juraj et al., 2009):

$$\varrho = \frac{X_t - x_s}{t - s}$$

Where X_t and X_s are the observed data at times t and s, respectively. Calculate the C_a parameter at the trust levels tested using the following formula:

$$C_a = Z1-\partial/2*\sqrt{Var(s)}$$

Where z is the standard normal distribution statistic, this statistic is considered 1.96 and 2.58 for 95% and 99% confidence levels, respectively. Finally, the upper and lower confidence limits are calculated using the following formula:

$$M_1 = \frac{N - C_a}{2}$$

$$M_2 = \frac{N + C_a}{2}$$

N is the number of slopes calculated in the first part. Previous studies have investigated hazy days to discover the existing trend of the haze phenomenon. But in this study, the unit intended for measuring haze is the synop, which is recorded every three hours.

The Mann-Kendall method is a non-parametric method that examines the presence or absence of change in parameters in a time series (Mann 1945; Kendal 1975). A factor that affects trend detection in a series is the presence of positive or negative autocorrelation (Yue *et al*. 2003; Novotny and Stefan, 2007). The statistics (S) is defined as:

$$S = \sum_{k-1}^{n-1} \sum_{j=k+1}^{n} sgn(x_j - x_k)$$

Where *N* is the number of data points. Assuming (xj – xi) = θ, the value of sgn (θ) is computed as follows:

$$\text{Sgn}(x) = \begin{cases} +1 \quad if \quad (x_i - x_k) > 0 \\ 0 \quad if \quad (x_i - x_k) = 0 \\ -1 \quad if \quad (x_i - x_k) < 0 \end{cases}$$

This statistic represents the number of positive differences minus the number of negative differences for all the differences considered. For large samples (N > 10), the test is conducted using a normal distribution, with mean and variance as follows:

$$\text{Var} = \frac{n(n-1)(2n+5) - \sum_{i=1}^{m} t(t-1)(2t+5)}{18}$$

Here n is the number of tied (zero difference between compared values) groups, and t_k is the number of data points in the k_{th} tied group. The standard normal deviate (Z statistics) is then computed as:

$$Z = \begin{cases} \frac{S-1}{\sqrt{var(s)}} \quad if \quad S > 0 \\ 0 \quad if \quad S = 0 \\ \frac{S+1}{\sqrt{var(s)}} \quad if \quad S < 0 \end{cases}$$

Stepwise linear regressions were used for three-hour $PM_{2.5}$ concentrations over Tehran to estimate the relative contribution of each meteorological parameter to the variations in wintertime $PM_{2.5}$ concentrations (as the primary cause of NHAZEs). Regressors include normalized 3-h WS (m s^{-1}), T (c), RH (%), and SLP (hPa). 3-h wintertime $PM_{2.5}$ concentrations were used as the dependent variable in the regression model. Since the data measurement scale was different, the Min-Max normalization method was used to change the scale of data and put them in the numeric range of (0, 1). The min-max method can be expressed as follows (Zhao et al., 2021):

$$x \text{ (normalized)} = \frac{x - \min(x)}{\max(x) - \min(x)}$$

Some other statistical methods are used in this study, including Pearson correlation analysis to determine the correlation significance of the data (Zhao et al., 2020; Zhang et al., 2015) and a 10-year Gaussian low-pass filter to evaluate the interannual variability.

2.6. Interpolation of NHAZEs and $PM_{2.5}$

The spatial distribution of $PM_{2.5,}$ and NHAZES have been depicted using inverse distance weighted (IDW) interpolation. The basic principle of IDW interpolation is to use a weighted linear combination set of sample points, and it counts on both statistical and mathematical methods to construct surfaces and predict unmeasured points (Khouni et al, 2021). Since IDW is a weighted distance average, the average cannot be greater than the highest or less than the lowest input (ArcGis 10.8 Desktop Help, 2021). The frequency of haze recorded at a station includes a wide area (not just around the station) due to the large-scale occurrence of this phenomenon. Previous research on air pollution and pollutant concentrations has used IDW method (e.g., Ranjbar and Bahak, 2019).

3. Results

3.1. Temporal changes in NHAZEs, $PM_{2.5}$ and visibility

The time series of annual and winter mean NHAZEs in Tehran are presented in Figure 3, showing a marked interannual variability of NHAZEs. The Gaussian low-pass filter clearly shows 5 phases for 1990-2020: (i) a significant decline with a rate of -50.7 synops year $^{-1}$ on an annual scale ($p<0.01$) and -18.2 synops year $^{-1}$ in winter ($p<0.05$) from 1990 to 1996; (ii) a significant increase with a rate of +8 synops year $^{-1}$ on an annual scale ($p<0.05$) for 1997-2001, and +4.6 synops year $^{-1}$ in winter ($p>0.05$) from 1997 to 2005; (iii) a significant decrease with a rate of -12.5 synops year $^{-1}$ on an annual scale($p<0.05$) for 2002-2012, and -3.6 synops year $^{-1}$ in winter ($p<0.05$) from 2006 to 2011; (iv) a non-significant increase with a rate of +12.7 synops year $^{-1}$ on an annual scale for 2013-2016, and +7.5 synops year $^{-1}$ in winter ($p<0.01$) for 2012-2015; and (v) a non-significant decrease with a rate of -5.06 synops year $^{-1}$ on an annual scale, and -6.06 synops year $^{-1}$ in winter from 2016-2020. For the entire series, the winter NHAZEs displayed an overall significant ($p<0.05$) decreasing trend of -0.5 synops year $^{-1}$, with an average of 189 synops per season, and -3.5 synops year $^{-1}$ ($p<0.05$) on the annual scale, with an average value of 386 synops per year. Since haze occurs more frequently in winter, the interannual variations of annual NHAZEs resemble the winter NHAZEs.

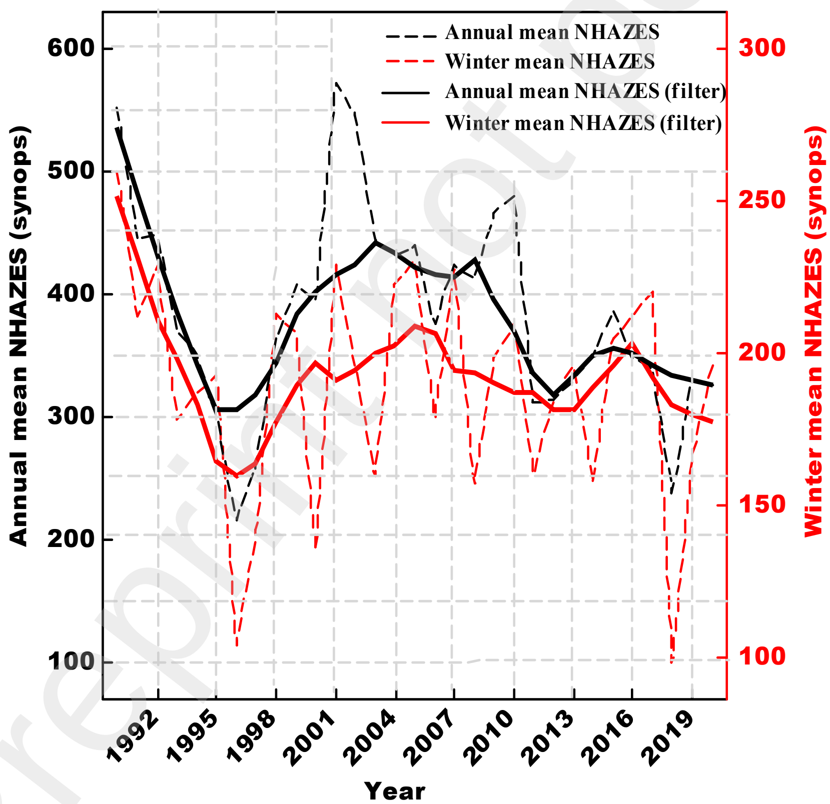

Figure 3: The time series of annual (black line) and winter (red line) NHAZEs over Tehran for 1990–2020. A 10-year Gaussian low-pass filter is drawn to highlight the interannual variability.

Figure 4 shows the annual and winter time series of average NHAZEs and $PM_{2.5}$ concentrations for 2013 – 2020. We found a strong and significant (p<0.05) positive relationship between both parameters in winter (R= 0.81) and annually (R= 0.55). This demonstrates that the interannual variability of both parameters was closely linked to each other (whit an exception in 2020). In particular, the lowest $PM_{2.5}$ concentrations and NHAZEs occurred in 2014 and 2018 in winter, whereas the highest one took place in 2017.

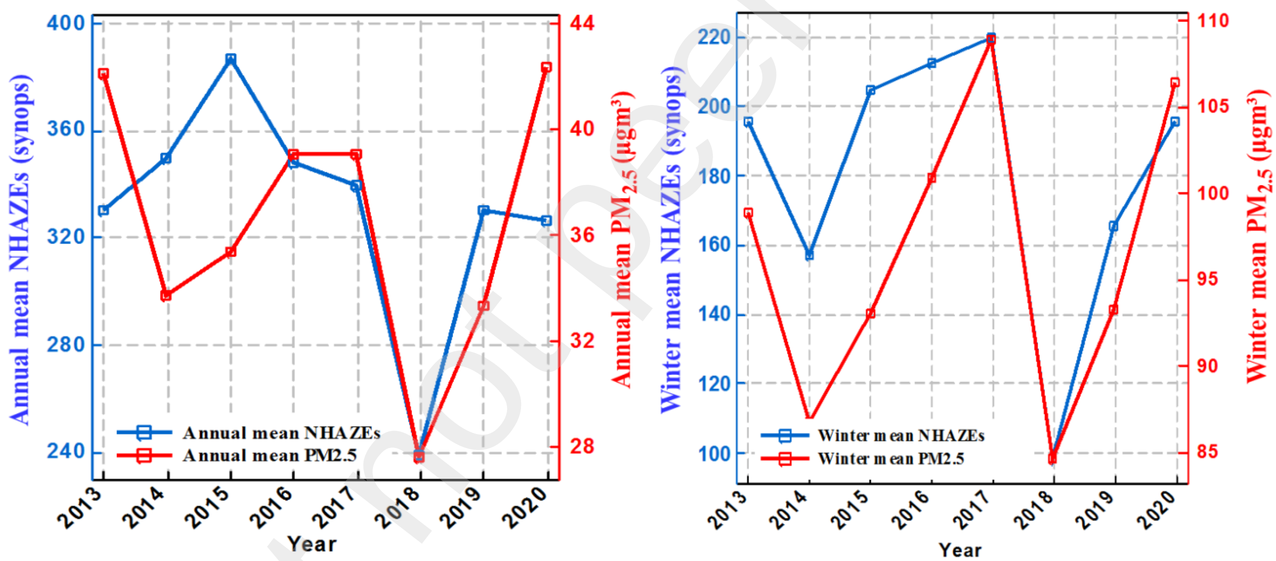

Figure 4: Annual and winter time series of average NHAZEs and $PM_{2.5}$ concentrations for 2013-2020.

Figure 5 presents the time series of observed annual and winter mean visibility and NHAZEs over Tehran for 1990-2020. Overall, the annual and winter mean visibility showed a significant increasing trend of +6.5 m year $^{-1}$ (p<0.05) and +29.2 m year $^{-1}$ (p<0.05) for 1990-2020, respectively. This increase in visibility is in line with the opposite decrease shown by NHAZEs.

In addition, the average of visibility was estimated in 9,244.3 m year $^{-1}$ (annual) and 7,834.1 m year $^{-1}$ (winter) for the entire 31-year period. Regarding the interannual variability, the winter mean visibility clearly displayed an opposite trend behavior compared with NHAZEs (R= -0.55 ; p<0.01), which experienced five changing phases: (i) an increase with a rate of +79.8 m year $^{-1}$ (non-significant) from 1990 to 1998; (ii) a decline with a rate of -172.98 m year $^{-1}$ (non-significant) from 1999 to 2004; (iii) an increase with a rate of +228 m year $^{-1}$ (p<0.01) from 2005 to 2010; (iv) a decline with a rate of -6.5 m year $^{-1}$ (non-significant) from 2011 to 2015; and (v) an increase with a rate of +345.28 m year $^{-1}$ (p<0.05) from 2016 to 2020. In the annual mean visibility, the Gaussian low-pass filter clearly shows 3 phases for 1990-2020: (i) an increase with a rate of +86.6 m year $^{-1}$ (non-significant) from 1990 to 1994; (ii) a decline with a rate of -116.6 m year $^{-1}$ (p<0.01) from 1995 to 2002; and (iii) an increase with a rate of +31.9 m year $^{-1}$ (p<0.01) from 2003 to 2020.

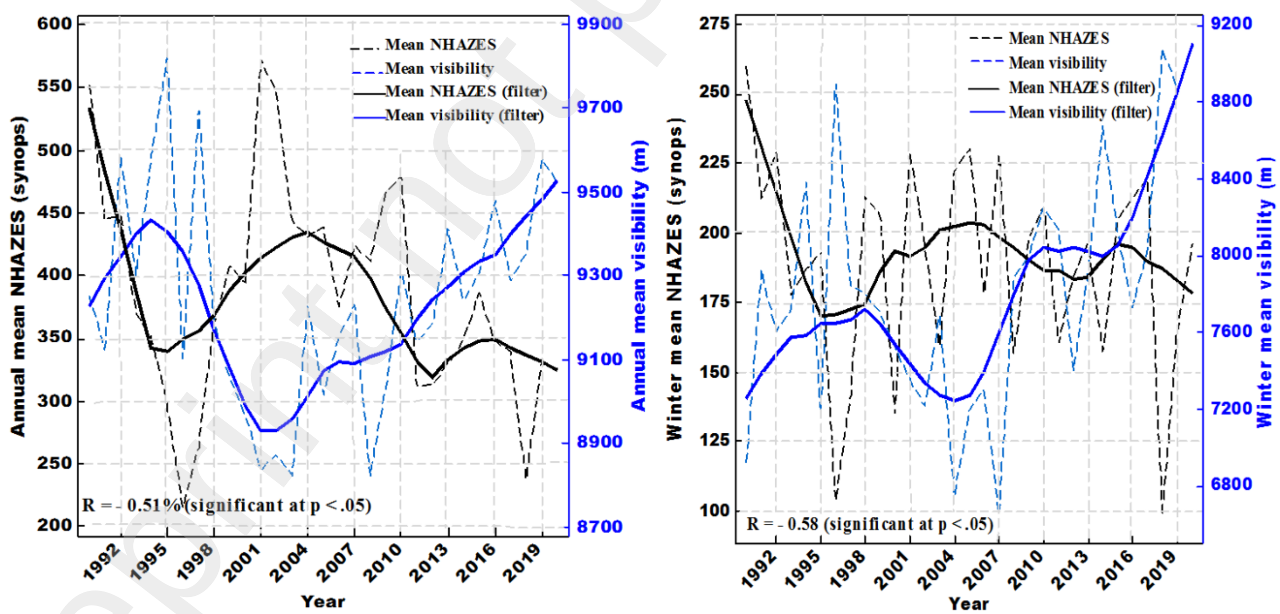

Figure 5: The time series of annual and winter mean NHAZEs (black line) and visibility (blue line) averaged over Tehran for 1990–2020. A 10-year Gaussian low-pass filter is drawn to highlight the interannual variability.

3.2. Spatial means in NHAZEs, $PM_{2.5}$ and visibility

The spatial distribution of the annual and winter mean NHAZEs, $PM_{2.5}$ concentrations and visibility has been depicted in Figure 6. Figures 6a (annual) and 6b (winter) show that the mean NHAZEs in Tehran reaches the highest value at the Mehrabad Airport station, in the western part of the study area, and the lowest one in Shemiran station in the northeast of Tehran. In addition to the Mehrabad Airport station, with a winter and annual averages of 289 and 616 NHAZEs, respectively, the Geophysics station also has a high frequency of this phenomenon with winter mean of 230 and annual mean of 574 NHAZEs. As can be seen in the Figures 6c and 6d, the highest amount of visibility occurs in areas with low NHAZEs and vice versa. Figures 6e and 6f show that the highest concentrations of $PM_{2.5}$ were found over the west and southwest of the region, where industries have developed quickly compared with other areas in Tehran. In contrast, the high-elevation northern areas have low $PM_{2.5}$ concentrations and high atmospheric visibility. Overall, the areas with the highest frequency of NHAZEs and highest concentrations of $PM_{2.5}$ have the lowest atmospheric visibility.

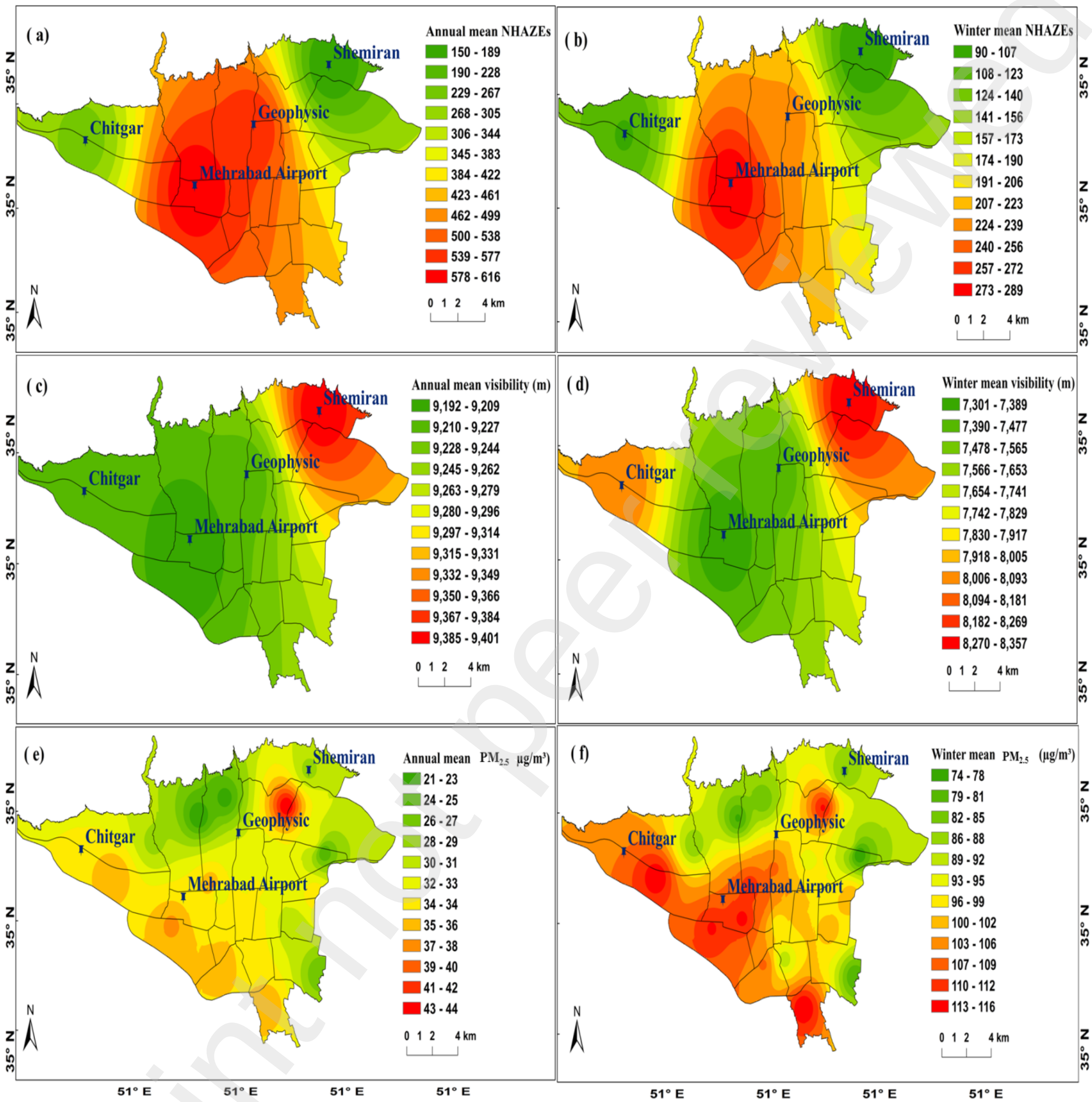

Figure 6: Spatial distribution of annual and winter mean NHAZEs (synops) (a and b); visibility (m) (c and d); and $PM_{2.5}$ concentrations (µg/m3) (e and f) in Tehran averaged over 1990–2020 (except for $PM_{2.5}$, 2013-2020).

3.3. Spatial trends in winter NHAZEs and visibility

Figures 7 focuses on the spatial distribution of winter trends in NHAZEs and visibility for 1990-2020, which are no significant in 80% of the study area. A non-significant increasing trend in NHAZEs (2 synops year $^{-1}$) was observed in the northern parts of the region, while central areas of Tehran showed a non-significant decreasing trend (-1.9 and -0.6 synops year $^{-1}$). This strong spatial variability in trends is shown e.g. by the non-significant decreasing trend at Mehrabad Airport station (-1.4 synops year $^{-1}$), while the Chitgar station (located west of the city, at 13 km from the airport) showed a significant and highest increasing trend of NHAZEs (+6 synops year $^{-1}$, $p<0.05$). The rate of winter NHAZEs changes varies between -1.9 and +8.6 synops year $^{-1}$ in the measuring stations. In contrast to NHAZEs, spatial trends of horizontal visibility are positive and significant in most parts of the study area; except for the Shemiran station located in the northeast of Tehran, which displayed a non-significant decreasing trend. Overall, the rate of changes for the winter visibility varies between -4.0 and +54.5 m year $^{-1}$ in different places.

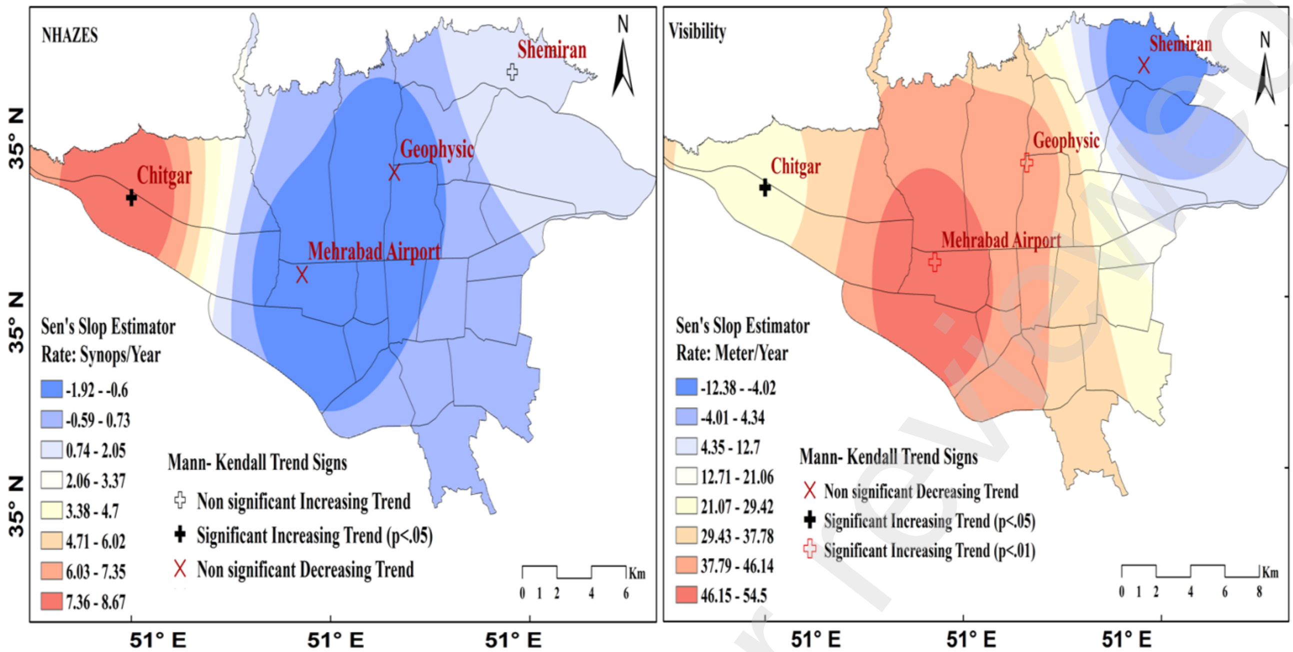

Figure 7: Spatial distribution of the sign, statistical significance and trends of winter NHAZEs and visibility in Tehran for 1990-2020.

3.4. Meteorological conditions influencing winter NHAZEs, $PM_{2.5}$ and visibility

To identify atmospheric conditions associated with winter NHAZEs and explain how these conditions differ from non-NHAZEs, Figure 8 presents the meteorological parameters under both situations. T in NHAZEs is higher on average than in non-NHAZEs, and it showed an increasing trend for NHAZEs (+0.05°C year $^{-1}$; p<0.05) of a smaller magnitude than in non-NHAZEs (+0.06°C year $^{-1}$; p<0.01) for 1990-2020. WS in NHAZEs is lower on average than in non-NHAZEs, and the increasing trend for NHAZEs (+0.04 m s^{-1} year $^{-1}$; p<0.01) is higher than for non-NHAZEs (+0.03 m s^{-1} year $^{-1}$; p<0.01), which has reduced NHAZEs in recent years. The RH has the same behavior as WS, with lower values on average in NHAZEs than in non-NHAZEs. The decrease in RH started from 1998, being the rate of change of this decrease in NHAZEs (-0.35% year $^{-1}$; p< 0.01) smaller than in non-NHAZEs (-0.45% year $^{-1}$; p< 0.01). SLP in NHAZEs is higher on average than in non-NHAZEs, and it showed a non-significant decreasing trend for NHAZEs (-0.01 hPa year $^{-1}$), and a non-significant increase in non-NHAZEs (0.003 hPa year $^{-1}$) for 1990-2020. Overall, we found that meteorological parameters differ between NHAZEs and non-NHAZEs, with high T, weak WS, low RH and high SLP dominating days with haze pollution across Tehran in winter.

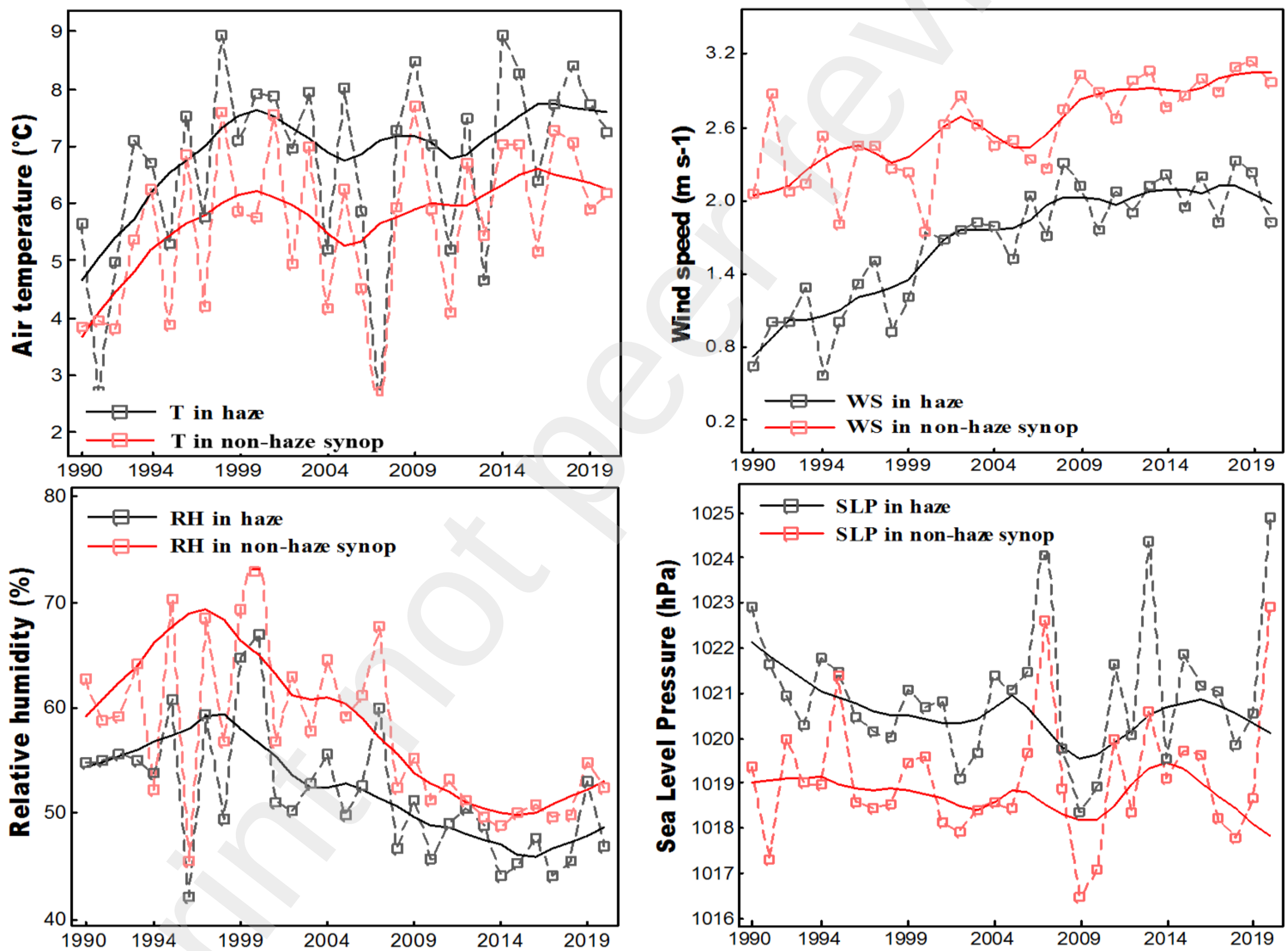

Figure 8. The mean winter air temperature (T), wind speed (WS), relative humidity (RH), and sea level pressure (SLP) of NHAZEs and non-NHAZEs in Tehran for 1990-2020. A 10-year Gaussian low-pass filter is drawn to highlight the interannual variability.

Table 3 summarizes the regression coefficients for the stepwise regression models. The regression coefficient for WS was negative (-0.30), indicating that decreases in WS led to increases in $PM_{2.5}$ concentrations. The T (+0.25) and SLP (+0.25) had a positive regression coefficient, which indicates the direct relationship of these variables to the $PM_{2.5}$ concentrations; that is, the increase in the T and SLP increased the $PM_{2.5}$ concentrations. The noteworthy point is the low regression coefficient for the relative humidity (0.09), which shows the small effect of this variable on NHAZEs. Therefore, high T and SLP, weak WS, and (almost low RH), enhance high $PM_{2.5}$ concentrations, resulting in strong haze events. Regression analysis showed that meteorological variables explain 30% of $PM_{2.5}$ concentrations, with WS (R^2 = -30%) having the highest impact on NHAZEs in the long term, and $PM_{2.5}$ concentrations explain 65% of NHAZEs.

Table 3: Regression Coefficients for Stepwise Linear Regression Models Performed with Spatially Averaged Meteorological Variables and $PM_{2.5}$ Concentrations for 4 synoptic meteorological stations in Tehran

	Regression Coefficients			
Meteorological Parameters	Chitgar (West of Tehran)	Geophysic (Center of Tehran)	Mehrabad Airport (Center of Tehran)	Shemiran (Northeast of Tehran)
WS (ms^{-1})	-0.20	-0.17	-0.30	-0.15
T (°C)	0.32	0.33	0.19	0.19
RH (%)	0.14	0.27	0.23	0.06
SLP (hPa)	0.24	0.14	0.21	0.22

Lastly, to better understand the extent of the impact of meteorological conditions on the haze events in Tehran, we analyzed three time periods based on the temporal variations in NHAZEs (see Figure 3). We selected the periods with relatively low NHAZEs, that is, 2006-2011 (Period

1), large NHAZEs, that is, 2012-2016 (Period 2), and again low NHAZEs that is, 2017–2020 (Period 3) for comparison. There were noticeable differences in the means of the four meteorological parameters (i.e., T, WS, RH, and SLP) among the periods (Table 4). Moreover, the standard deviations of the four meteorological parameters were larger in Period 1 compared to Periods 2 and 3, demonstrating that the meteorological conditions had larger variations during the winters for 2006–2011. RH decreased significantly (p<0.05), whereas T increased significantly in Period 2 compared to Period 1. RH was higher, whereas T was lower in Period 3 compared to Period 2. These changes may explain the increased role of climate and meteorological conditions on haze pollution after 2013 in Tehran.

Table 4: The mean and standard deviations in the meteorological parameters for the different time periods in the Tehran metropolis

Time period → / Meteorological parameters ↓	Period 1 (2006-2011)		Period 2 (2012-2016)		Period 3 (2017-2020)	
	Mean	SD	Mean	SD	Mean	SD
WS (m/s)	1.62	0.18	1.78	0.02	1.77	0.14
T (°C)	4.43	2.02	5.94	1.03	5.79	0.63
RH (%)	59.30	4.05	54.77	1.27	56.30	2.12
SLP	1019.76	2.29	1020.14	1.26	1019.46	1.03

3.5. Winter haze case study: January 2017

According to Figure 3, the highest frequency of NHAZEs (during last decade), occurred in winter 2017, particularly in January. Figure 9 presents the daily series of $PM_{2.5}$ measurements, concentrations of gaseous pollutants (SO2, CO, NO2, and O3), and meteorological parameters from the 1st till 30st January 2017 (For January 31, the data related to pollutants was not recorded). $PM_{2.5}$ concentrations were ranged from 46 to 177 µgm³. The highest value of $PM_{2.5}$ was recorded at 9:00 (i.e., rush hours in Tehran) on January 9 (177µg/m³), when RH was 30 % and O3 was 11µg/m³. The T was high (10.8 °C), and WS was at 2 m s^{-1} throughout that day. The NO2 value was 45µg/m³, which was considerably higher than the average (25.8µg/m³). On January 9, the highest amount of $PM_{2.5}$ was recorded when the amount of T, SLP, SO2, CO, and NO2 were high, and the WS, RH, and O3 were low. Conversely, the minimum value of $PM_{2.5}$ was at lower SO2 (10µg/m³), CO (1 mg/m³), and a higher concentration of O3 (24.0 µg/m³). We also detected that CO levels rise a few hours after $PM_{2.5}$ levels increase, reaching 10 mg/m3. Since SO2, CO, and NO2 were primary emissions from similar sources such as coal combustion and industrial processes, they showed similar variations in their concentrations. However, O3 showed the opposite trend.

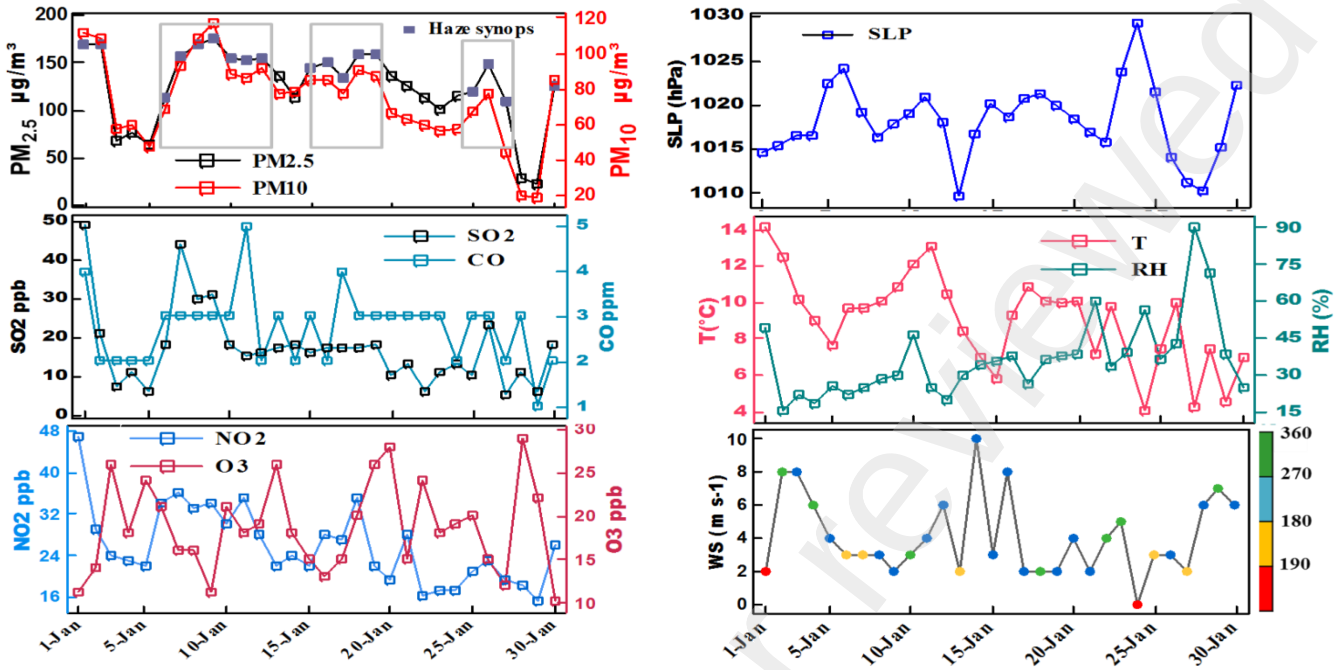

Figure 9. Time series of daily means of $PM_{2.5}$ concentrations, gaseous pollutants (SO2, CO, NO2, and O3), T, SLP, RH, and WS (colored by wind direction, note 0, 90, 180, and 270 refer to northerly, easterly, southerly and westerly winds, respectively). Note that the gray rectangles represent the days with the highest $PM_{2.5}$ concentrations and NHAZEs (note that the synop associated with haze are marked with blue rectangles).

As part of our analysis of January's pollution, we identified three polluted periods with different meteorological conditions (based on the criteria that the concentration of $PM_{2.5}$ is higher than 120 ug/m3 and at least 4 out of 8 synop in a day have reported haze). Table 5 summarizes the average, minimum, and maximum values of pollutant gases and meteorological parameters for the three polluted periods, the clean periods (which are recorded between polluted periods), and the whole month of January. The average RH and WS in period 1 are low compared to periods 2 and 3. The highest T was also recorded in the period 1. There was no noticeable difference in SLP during these periods. Except for O3, which experienced its maximum value in period 2, the other pollutants had the highest values during period 1. The duration of haze was longer under low RH, weak WS, and high T (the first period lasted seven days). In periods 2 and 3, with the change in meteorological parameters (increased RH and WS and decreased T), the concentration of pollutants decreased, and these periods lasted shorter, indicating the key role played by meteorological parameters in controlling haze in Tehran.

Table 5: Comparison of major pollutants and meteorological parameters among three pollution periods and the clean period in January 2017

	Polluted period1 (6th 6:00 – 12th 9:00)			Polluted period2 (16th 6:00 – 20th 18:00)			Polluted period3 (24th 9:00 – 27th 21:00)			Clean period			January (total)		
	Ave.	Min	Max	Ave.	Min	Max	Ave.	Min	Max	Ave.	Min	Max	Ave.	Min	Max
$PM_{2.5}$ (ug/m3)	155.7	114.0	177.0	137.4	113.0	159.0	120.2	100.0	149.0	77.0	46.0	100.0	133.0	46.0	177.0
PM_{10} (ug/m3)	95.2	69.0	117.0	77.0	60.0	91.0	64.5	44.0	85.0	55.3	48.0	60.0	78.5	44.0	117.0
SO2 (ppb)	25.9	15.0	49.0	14.7	6.0	18.0	13.3	5.0	23.0	8.7	6.0	11.0	17.1	5.0	49.0
NO2 (ppb)	32.8	22.0	47.0	24.6	16.0	35.0	20.5	17.0	26.0	19.8	15.0	24.0	25.8	15.0	47.0
O3 (ppb)	17.3	11.0	26.0	19.3	13.0	28.0	15.7	10.0	20.0	22.8	18.0	29.0	18.7	10.0	29.0
CO (ppm)	3.1	2.0	5.0	2.9	2.0	4.0	2.5	2.0	3.0	2.2	1.0	3.0	2.7	1.0	5.0
T (°C)	7.0	0.5	14.6	5.7	1.0	10.8	5.1	0.4	9.9	4.4	-3.4	12.5	5.4	-3.4	14.6
RH (%)	44.2	21.0	70.0	50.2	26.0	77.0	51.5	36.0	77.0	51.6	15.0	93.0	49.5	15.0	93.0
WS (ms^{-1})	1.9	0.0	6.0	1.9	0.0	4.0	2.6	0.0	6.0	3.1	0.0	10.0	2.5	0.0	10.0
SLP (hPa)	1019	1009	1027	1021	1015	1024	1021	1010	1031	1018	1010	1032	1019	1009	1032

As mentioned above, January 9th 2017 recorded the peak of pollution in the Tehran metropolis. The $PM_{2.5}$ concentrations reached the highest value (177 μg/m³), and all eight synops (once every three hours) reported haze across all stations. Figure 10a displays the SLP on that day, showing a high-pressure system (<1025 mb) located in the northwest of Iran, with the studied area dominated by its clockwise currents so that the T (Figure 10b) of the high-pressure core reached -4°C and varied between 4 and 8°C in Tehran. The dominance of high pressure conditions caused the loss of humidity and increase in T due to the subsidence of the air to the lower layers of the atmosphere. Combined maps of geopotential height and omega level at 850 and 700 hPa (Figures 10c and 10d) indicate the formation of a low pressure over the Mediterranean. The study area was affected by the eastern part of this low pressure system, which moved warm air from low latitudes to Iran driven by the counterclockwise movement. The positive omega values indicate stability. Moreover, the combined maps of specific humidity and wind vector at 850 and 700 hPa (Figures 10e and 10f) also showed patches of low specific humidity (4 to 6 g/kg) around Tehran. The dominance of weak southerly and southwesterly winds were also responsible of this extreme pollution event, as suspended particles were trapped in Tehran.

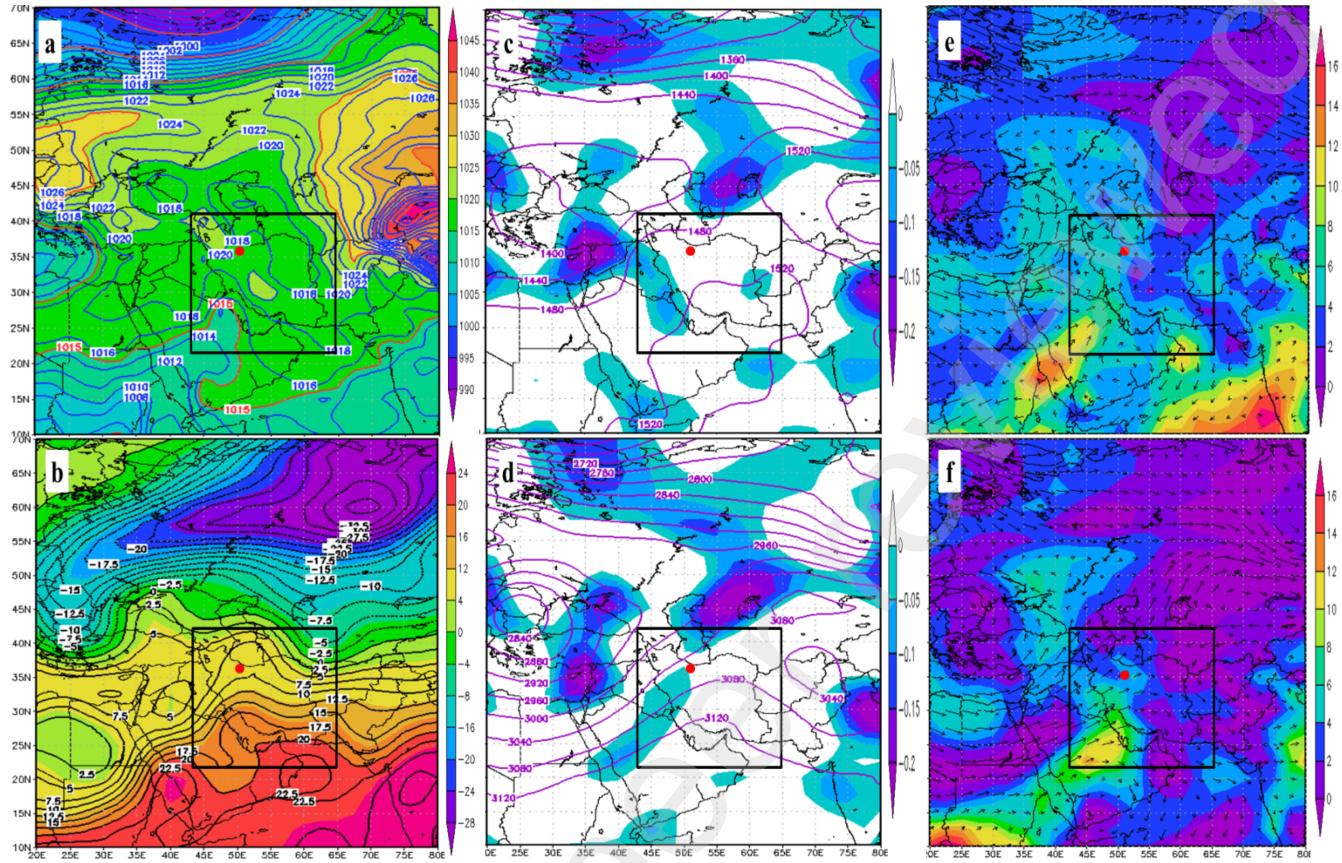

Figure 10: Map of SLP (a) and T (surface) (b), geopotential height and omega at 850 (c) and 700 (d) hPa, and specific humidity and wind vector map at 850 (e) and 700 (f) hPa for January 9^{th} 2017. Note that in the maps above, the measurement units are as follows: Slp (hPa), T (°C), omega (Pa/s), and specific humidity (g/kg). The black rectangle shows the location of Iran and the red dot shows the location of Tehran.

4. Discussion

Haze pollution is hazardous to human health and economic development (Hao et al., 2021; Gan et al., 2021; Feng and Yuan., 2021; Liu et al., 2019). Further research to better assess this phenomenon in highly polluted cities such as Tehran (Iran) is essential to develop regional pollution control strategies. Using observations of $PM_{2.5}$ concentrations, NHAZEs based on visibility and relative humidity and meteorological observations, this research investigated for the first time the spatio-temporal variation of haze pollution, its relationship with gaseous pollutants and meteorological conditions over Tehran for 1990-2020. The trend in NHAZEs revealed significant (p<0.05) decline of -3.5 synops year $^{-1}$ annually and -0.5 synops year $^{-1}$ in winter (p<0.05) across Tehran for 1990–2020. The long-term NHAZEs time series showed five short phases of change, denoting a marked interannual variability. Considering that $PM_{2.5}$ data was not recorded before 2013, a major constraint of this study was to quantify NHAZEs changes in relation to $PM_{2.5}$ for the entire period; we alternatively focused on the relationship between NHAZEs and meteorological variables for investigating the drivers behind their variations for the early decades. Moreover, the visibility and NHAZEs had a relatively high and negative correlation coefficient (-0.55, p<0.01), i.e. with an opposite trend behavior and showing five opposite changing phases (Yang et al., 2016; Zhao et al., 2020). Overall, the annual and winter mean visibility both showed a significant increasing trend from 1990 to 2020, with a rate of +6.5 m (p < 0.05) and +29.2 m (p <0.05), respectively.

The investigation of the relationship between $PM_{2.5}$, the principal cause of haze, and NHAZEs evidenced a strong and positive correlation (R= 0.81, p<0.01) for 2013-2020. However, we found a exception in 2020 as high $PM_{2.5}$ concentrations and low NHAZEs occurred, which could be explained by the changes in relative humidity or in the chemical components of $PM_{2.5}$ affecting aerosol optical characteristics (He et al., 2018). For this short period, we found that the increasing tendency of $PM_{2.5}$ concentrations is consistent with the overall increase reported by the Environmental Research Institute - Air Pollution Research Center (https://ier.tums.ac.ir ; Tehran Air Quality Control Company, 2021, https://air.tehran.ir/; last accessed 15 October, 2022)

Examining the spatial variation of NHAZEs, $PM_{2.5}$ concentrations, and visibility, we revealed large differences in different regions across Tehran metropolis. The highest concentrations of NHAZEs and $PM_{2.5}$ were found at the west and southwest of the city, where industries have developed quickly over the last decades. Daytime traffic and population, car traffic, a lack of green space, and the existence of passenger terminals are all factors that contribute to high $PM_{2.5}$ emissions in the region (International Communication and Relations Center of Tehran Municipality, 2019, https://ccia.tehran.ir/; last accessed 15 October, 2022; Heydari et al., 2020; Ehsani and Bigdeli, 2021). Also, the north, east, and northeast regions had the lowest concentrations of $PM_{2.5}$. The northern and eastern areas of Tehran have cleaner air due to more green spaces per capita and the use of new cars with fewer emissions (Alavi et al., 2020). However, the visibility varied according to the amount of $PM_{2.5}$ concentrations and NHAZEs in different parts of Tehran; that is, the regions with the highest $PM_{2.5}$ emissions had the lowest horizontal visibility. Since most industries have been established in the west of Tehran, and the prevailing winds in Tehran are the westerlies, pollutants move towards the city center, resulting in the accumulation of primary and secondary pollutants in the west and central parts of the city.

Exploring the role of meteorological parameters in the occurrence of NHAZEs in Tehran revealed that WS had a significant effect, with a regression coefficient of -0.30 ($p<0.05$). Over the entire 31 years, NHAZEs were observed when the T was high and the RH and WS were low. The intensity, duration, and prevalence of NHAZEs were high during the establishment of anticyclonic conditions, which caused the stability of the air. All meteorological variables played a role in the decreasing and increasing periods of NHAZEs, in which the WS had the greatest impact. As a result, in recent years, with the increase in wind speed, we observed a decline in

NHAZEs and an increase in visibility. This is consistent with the recent reversal of terrestrial surface winds globally (Zeng et al. 2019) or in nearby countries like Saudi Arabia (Azorin-Molina et al. 2018), but there is a lack of research on changes of WS across Iran.

Simultaneous analysis of pollutant gases and $PM_{2.5}$ concentrations (the primary cause of haze) showed that the highest amount of $PM_{2.5}$ was recorded when the amounts of RH, SO2, CO, and NO2 were high but the WS and O3 were low. Conversely, the minimum value of PM2.5 was at lower RH, SO2, and CO and a higher concentration of O3. Many previous studies have confirmed these events (Yang et al., 2007; Tai et al., 2010; Xu et al., 2011; Li et al., 2017). Considering the high concentration of $PM_{2.5}$ in recent years, it can be concluded that the reason behind the reduction of NHAZEs is associated with the favorable meteorological conditions (especially the increasing tendency of WS), which enhance the dispersion of pollutants.

In general, Tehran is a polluted city in Iran surrounded by the Alborz Mountain Range, which also affects the dispersion pattern of pollutants (Safavi and Alijani, 2006; Ashrafi, 2012). The government's primary concern should be to control pollution emissions effectively. Attempting to outlaw the use of fuels like mazut, kerosene, and diesel in all industries should be among the government's main focuses. In the future, the government and researchers must investigate human factors and large-scale atmospheric patterns affecting the haze and its characteristics and formation mechanisms in the Tehran metropolis.

5. Conclusions

The main findings of this research are as follows:

1. A marked interannual variability in the number of haze synop (NHAZEs) is found in Tehran, with a significant decreasing trend for 1990-2020. On the contrary, visibility has improved as revealed by the significant increasing trend found in the last three decades.

2. Strong spatial differences in NHAZEs are observed across the region, with the highest NHAZEs detected in the western and central areas of the city, where industries have developed quickly over the years.

3. The intensity, duration, and prevalence of NHAZEs were high under anticyclonic conditions. The meteorological variables can explain 30% of the interannual variability of NHAZEs and 65% of $PM_{2.5}$ concentrations, with the WS exerting the highest impact.

4. Wind speed is increasing in Tehran for 1990-2020, which could partly explain the significant decline in NHAZEs and the significant increase in visibility.

5. The small regression coefficient of meteorological variables and the high correlation of NHAZEs with $PM_{2.5}$ concentrations indicate the relevance of investigating the influence of human resources on haze events in Tehran; more pollution monitoring stations are needed.

Acknowledgements

The authors would like to acknowledge the Iranian Meteorological Organization (IRIMO), Tehran Air Quality Control Company, and the European Centre for Medium-Range Weather Forecasts (ECMWF), for free access to the data. C. A-M. was supported by VENTS (GVA-AICO/2021/023), the CSIC Interdisciplinary Thematic Platform (PTI) Clima (PTI-CLIMA), and the "Unidad Asociada CSIC-Universidad de Vigo: Grupo de Física de la Atmosfera y del Océano".

This research did not receive any specific grant from funding agencies in the public, commercial, or not-for-profit sectors.

References

Aditya, F., Gusmayanti, E., Sudrajat, J., Rainfall trend analysis using Mann-Kendall and Sen's slope estimator test in West Kalimantan. *IOP Conference Series: Earth and Environmental Science*, IOP Publishing (2021), p. 012006. http://DOI 10.1088/1755-1315/893/1/012006

Alavi, C., Kianejad, S, Sabbagh, S.A., 2019. Preparation of Air Pollution Mapping by Interpolating Kriging Method in GIS, Case Study: Tehran Metropolis, Journal of Urban Ecology Researches. 10, 171-184.

Alexandersson, H., 1986. A homogeneity test applied to precipitation data, Journal of climatology. 6, 661-675. https://doi.org/10.1002/joc.3370060607

Ali-Taleshi, M.S., Bakhtiari, A.R., Hopke, P.K., 2022. Particulate and gaseous pollutants in Tehran, Iran during 2015-2021: Factors governing their variability. Sustainable Cities and Society. 87, 104183. https://doi.org/10.1016/j.scs.2022.104183

Ashrafi, K., 2012. Determining of spatial distribution patterns and temporal trends of an air pollutant using proper orthogonal decomposition basis functions. Atmospheric Environment. 47, 468-476. https://doi.org/10.1016/j.atmosenv.2011.10.016

An, Z., Huang, R.-J., Zhang, R., Tie, X., Li, G., Cao, J., Zhou, W., Shi, Z., Han, Y., Gu, Z., 2019. Severe haze in northern China: A synergy of anthropogenic emissions and atmospheric processes. Proceedings of the National Academy of Sciences. 116, 8657-8666. https://doi.org/10.1073/pnas.1900125116.

Azorin-Molina, C., Menendez, M., McVicar, T.R., Acevedo, A., Vicente-Serrano, S.M., Cuevas, E., Minola, L., Chen, D., 2018. Wind speed variability over the Canary Islands, 1948–2014: focusing on trend differences at the land–ocean interface and below–above the trade-wind inversion layer. Climate Dynamics. 50, 4061-4081. DOI 10.1007/s00382-017-3861-0.

Azorin-Molina, C., Vicente-Serrano, S.M., McVicar, T.R., Jerez, S., Sanchez-Lorenzo, A., López-Moreno, J.-I., Revuelto, J., Trigo, R.M., Lopez-Bustins, J.A., Espírito-Santo, F., 2014. Homogenization and assessment of observed near-surface wind speed trends over Spain and Portugal, 1961–2011. Journal of Climate. 27, 3692-3712. https://doi.org/10.1175/JCLI-D-13-00652.1

Azorin-Molina, C., Rehman, S., Guijarro, J.A., McVicar, T.R., Minola, L., Chen, D., Vicente-Serrano, S.M., 2018. Recent trends in wind speed across Saudi Arabia, 1978–2013: A break in the stilling. International Journal of Climatology. 38, e966-e984. https://doi.org/10.1002/joc.5423

Bross, I.D., 1958. How to use ridit analysis. Biometrics. 18-38.

Cohen, A.J., Brauer, M., Burnett, R., Anderson, H.R., Frostad, J., Estep, K., Balakrishnan, K., Brunekreef, B., Dandona, L., Dandona, R., 2017. Estimates and 25-year trends of the global burden of disease attributable to ambient air pollution: an analysis of data from the Global Burden of Diseases Study 2015. The Lancet. **389**, 1907-1918. https://doi.org/10.1016/S0140-6736(17)30505-6

Cunderlik, J.M., Ouarda, T.B., 2009. Trends in the timing and magnitude of floods in Canada. Journal of hydrology. 375, 471-480. https://doi.org/10.1016/j.jhydrol.2009.06.050

Ding, Y., Li, Q., Liu, Y., Zhang, L., Song, Y., Zhang, J., 2009. Atmospheric aerosols, air pollution and climate change. Meteorological Monthly. 35, 3-15.

Ding, Y., Liu, Y., 2014. Analysis of long-term variations of fog and haze in China in recent 50 years and their relations with atmospheric humidity. Science China Earth Sciences. 57, 36-46. https://doi.org/10.1007/s11430-013-4792-1

Doyle, M., Dorling, S., 2002. Visibility trends in the UK 1950–1997. Atmospheric Environment. 36, 3161-3172. https://doi.org/10.1016/S1352-2310(02)00248-0

Ehsani, A.H., Bigdeli, M., 2020. The PM2. 5 estimations over Tehran Using Remotely Sensed Aerosol Optical Depths Data. Journal of Climate Research. 1399, 99-108.

Feng, W., Yuan, H., 2021. Haze pollution and economic fluctuations: an empirical analysis of Chinese cities. Cleaner Environmental Systems. 2, 100010. https://doi.org/10.1016/j.cesys.2021.100010

Gan, T., Liang, W., Yang, H., Liao, X., 2020. The effect of Economic Development on haze pollution (PM2. 5) based on a spatial perspective: Urbanization as a mediating variable. Journal of Cleaner Production. 266, 121880. https://doi.org/10.1016/j.jclepro.2020.121880

Gan, T., Yang, H., Liang, W., 2021. How do urban haze pollution and economic development affect each other? Empirical evidence from 287 Chinese cities during 2000–2016. Sustainable Cities and Society. 65, 102642. https://doi.org/10.1016/j.scs.2020.102642

Guijarro, J.A., 2018. Homogenization of climatic series with Climatol. Reporte técnico State Meteorological Agency (AEMET), Balearic Islands Office, Spain. DOI: 10.13140/RG.2.2.27020.41604

Hao, Y., Niu, X., Wang, J., 2021. Impacts of haze pollution on China's tourism industry: A system of economic loss analysis. Journal of environmental management. 295, 113051. https://doi.org/10.1016/j.jenvman.2021.113051

He, C., Hong, S., Mu, H., Tu, P., Yang, L., Ke, B., Huang, J., 2021. Characteristics and Meteorological Factors of Severe Haze Pollution in China. Advances in Meteorology. 2021. https://doi.org/10.1155/2021/6680564

He, J., Gong, S., Zhou, C., Lu, S., Wu, L., Chen, Y., Yu, Y., Zhao, S., Yu, L., Yin, C., 2018. Analyses of winter circulation types and their impacts on haze pollution in Beijing. Atmospheric Environment. 192, 94-103. https://doi.org/10.1016/j.atmosenv.2018.08.060

Heydari, A., Mohammadi, M. Esmaeli, R., 2020. The relationship between the transportation of traffic load and the concentration of air pollutants in metropolises, 6rd International Conference new ideas in Agriculture, Environment and Tourism

Heger, M., Sarraf, M., 2018. Air Pollution in Tehran. http://hdl.handle.net/10986/29909

Hejazizadeh, Z., Pazhooh, F, Koohi, S., Jafari, F., 2017. Investigation of the relationship between synoptic patterns and the amount of suspended particles of pervasive pollutants in Tehran province, International Science and Research Journal of Iranian Geography Association, Vol.15, No. 53, P. 21-35.

Hyslop, N.P., 2009. Impaired visibility: the air pollution people see. Atmospheric Environment. 43, 182-195. https://doi.org/10.1016/j.atmosenv.2008.09.067

Kampa, M., Castanas, E., 2008. Human health effects of air pollution. Environmental pollution. 151, 362-367. https://doi.org/10.1016/j.envpol.2007.06.012

International Communication and Relations Center of Tehran Municipality, 2019

Kendall, M.G., 1975. Rank correlation methods.

Khouni, I., Louhichi, G., Ghrabi, A., 2021. Use of GIS based Inverse Distance Weighted interpolation to assess surface water quality: Case of Wadi El Bey, Tunisia. Environmental Technology & Innovation. 24, 101892. https://doi.org/10.1016/j.eti.2021.101892

Li, H., Ma, Y., Duan, F., He, K., Zhu, L., Huang, T., Kimoto, T., Ma, X., Ma, T., Xu, L., 2017. Typical winter haze pollution in Zibo, an industrial city in China: Characteristics, secondary formation, and regional contribution. Environmental Pollution. 229, 339-349. https://doi.org/10.1016/j.envpol.2017.05.081

Li, M., Yao, Y., Simmonds, I., Luo, D., Zhong, L., Pei, L., 2021. Linkages between the atmospheric transmission originating from the North Atlantic Oscillation and persistent winter haze over Beijing. Atmospheric Chemistry and Physics. 21, 18573-18588. https://doi.org/10.5194/acp-21-18573-2021

Liu, C., Chen, R., Sera, F., Vicedo-Cabrera, A.M., Guo, Y., Tong, S., Coelho, M.S., Saldiva, P.H., Lavigne, E., Matus, P., 2019. Ambient particulate air pollution and daily mortality in 652 cities. New England Journal of Medicine. 381, 705-715. DOI: 10.1056/NEJMoa1817364

Liu, H., Yue, F., Xie, Z., 2022. Quantify the role of anthropogenic emission and meteorology on air pollution using machine learning approach: A case study of PM2. 5 during the COVID-19 outbreak in Hubei Province, China. Environmental Pollution. 300, 118932. https://doi.org/10.1016/j.envpol.2022.118932

Mann, H.B., 1945. Nonparametric tests against trend. Econometrica: Journal of the econometric society. 245-259. https://doi.org/10.2307/1907187

Novotny, E.V., Stefan, H.G., 2007. Stream flow in Minnesota: Indicator of climate change. Journal of Hydrology. 334, 319-333. https://doi.org/10.1016/j.jhydrol.2006.10.011

Pishdad, E., Alijani, B., Aliakbari-Bidokhti, A.A., Akbari, M., 2020. Long Term Status Analysis of Major Air Pollutants and Determination of Air Pollution Periods in Tehran Metropolis. Journal of the Earth and Space Physics. 46, 355-376. doi: 10.22059/jesphys.2020.292565.1007177

Ramezani, N A., Alijani, B., borna, R.,2018. Explaining the Effects of Climate Elements in Tehran's Metropolis Air Quality. GeoRes. 33 (3) :154-169. doi: 10.29252/geores.33.3.154

Ranjbar, M., Bahak, B., 2019. Time and Space Changes of Air Pollutants Using GIS (case study: the northern half of Tehran). International Science and Research Journal of Iranian Geography Association, Vol.17, No.60, P. 73-85.

Raziei, T., 2017. Köppen-Geiger climate classification of Iran and investigation of its changes during 20th century. Journal of the Earth and Space Physics. 43, 419-439. https://www.researchgate.net/publication/308027173

Safavi, S., Alijani, B., 2006. Study of effective geographical factorsthe air pollution in Tehran city. Geogr Res J. 58, 99-112.

Shahbazi, H., Reyhanian, M., Hosseini, V., Afshin, H., 2016. The relative contributions of mobile sources to air pollutant emissions in Tehran, Iran: An emission inventory approach. Emission control science and technology. 2, 44-56. DOI 10.1007/s40825-015-0031-x

Shen, L., Jacob, D.J., Mickley, L.J., Wang, Y., Zhang, Q., 2018. Insignificant effect of climate change on winter haze pollution in Beijing. Atmospheric Chemistry and Physics. 18, 17489-17496. https://doi.org/10.5194/acp-18-17489-2018

Shi, P., Zhang, G., Kong, F., Chen, D., Azorin-Molina, C., Guijarro, J.A., 2019. Variability of winter haze over the Beijing-Tianjin-Hebei region tied to wind speed in the lower troposphere and particulate sources. Atmospheric Research. 215, 1-11. https://doi.org/10.1016/j.atmosres.2018.08.013

Tai, A.P., Mickley, L.J., Jacob, D.J., 2010. Correlations between fine particulate matter (PM2. 5) and meteorological variables in the United States: Implications for the sensitivity of PM2. 5 to climate change. Atmospheric environment. 44, 3976-3984. https://doi.org/10.1016/j.atmosenv.2010.06.060

Tan, J.-H., Duan, J.-C., Chen, D.-H., Wang, X.-H., Guo, S.-J., Bi, X.-H., Sheng, G.-Y., He, K.-B., Fu, J.-M., 2009. Chemical characteristics of haze during summer and winter in Guangzhou. Atmospheric Research. 94, 238-245. https://doi.org/10.1016/j.atmosres.2009.05.016

Torbatian, S., Hoshyaripour, A., Shahbazi, H., Hosseini, V., 2020. Air pollution trends in Tehran and their anthropogenic drivers. Atmospheric Pollution Research. 11, 429-442. https://doi.org/10.1016/j.apr.2019.11.015

Van, D.-A., Vu, T.V., Nguyen, T.-H.T., Vo, L.-H.T., Le, N.H., Nguyen, P.H., Pongkiatkul, P., Ly, B.-T., 2022. A Review of Characteristics, Causes, and Formation Mechanisms of Haze in Southeast Asia. Current Pollution Reports. 1-20. 10.1007/s40726-022-00220-z

Wang, J., Liu, Y., Ding, Y., 2020. On the connection between interannual variations of winter haze frequency over Beijing and different ENSO flavors. Science of the Total Environment. 740, 140109. https://doi.org/10.1016/j.scitotenv.2020.140109

Wei, K., Tang, X., Tang, G., Wang, J., Xu, L., Li, J., Ni, C., Zhou, Y., Ding, Y., Liu, W., 2020. Distinction of two kinds of haze. Atmospheric Environment. 223, 117228. https://doi.org/10.1016/j.atmosenv.2019.117228

World Bank staff based on data from the World Health Organization, (WHO) 2016.

World Meteorological Organization 2019 Guide to climatological practices, second edition.

Xiao, D., Li, Y., Fan, S., Zhang, R., Sun, J., Wang, Y., 2015. Plausible influence of Atlantic Ocean SST anomalies on winter haze in China. Theoretical and Applied Climatology. 122, 249-257. DOI 10.1007/s00704-014-1297-6

Xingqin, A., Yan, T., Shengquan, M. Zhaobin, S., Qing, H., 2015. Association between PM10 and respiratory hospital admissions in different seasons in heavily polluted Lanzhou city, Journal of Environmental Health. 77, 64-71.. https://www.jstor.org/stable/26330186.

Xu, W., Zhao, C., Ran, L., Deng, Z., Liu, P., Ma, N., Lin, W., Xu, X., Yan, P., He, X., 2011. Characteristics of pollutants and their correlation to meteorological conditions at a suburban site in the North China Plain. Atmospheric Chemistry and Physics. 11, 4353-4369. https://doi.org/10.5194/acp-11-4353-2011

Yang, L.-x., Wang, D.-c., Cheng, S.-h., Wang, Z., Zhou, Y., Zhou, X.-h., Wang, W.-x., 2007. Influence of meteorological conditions and particulate matter on visual range impairment in Jinan, China. Science of the Total Environment. 383, 164-173. https://doi.org/10.1016/j.scitotenv.2007.04.042

Yang, Y., Liao, H., Lou, S., 2016. Increase in winter haze over eastern China in recent decades: Roles of variations in meteorological parameters and anthropogenic emissions. Journal of Geophysical Research: Atmospheres. 121, 13,050-013,065. https://doi.org/10.1002/2016JD025136

Yasar, M., Lai, A.M., de Foy, B., Schauer, J.J., Arhami, M., Hosseini, V., 2020. Chemical speciation of PM2. 5 in Tehran: Quantification of dust contribution and model validation. Atmospheric Pollution Research. 11, 1839-1846. https://doi.org/10.1016/j.apr.2020.07.020

Ye, S., Ma, T., Duan, F., Li, H., He, K., Xia, J., Yang, S., Zhu, L., Ma, Y., Huang, T., 2019. Characteristics and formation mechanisms of winter haze in Changzhou, a highly polluted industrial city in the Yangtze River Delta, China. Environmental Pollution. 253, 377-383. https://doi.org/10.1016/j.envpol.2019.07.011

Yin, Z., Zhou, B., Chen, H., Li, Y., 2021. Synergetic impacts of precursory climate drivers on interannual-decadal variations in haze pollution in North China: A review. Science of the Total Environment. 755, 143017. https://doi.org/10.1016/j.scitotenv.2020.143017

Yue, S., Pilon, P., Phinney, B., 2003. Canadian streamflow trend detection: impacts of serial and cross-correlation. Hydrological Sciences Journal. 48, 51-63. https://doi.org/10.1623/hysj.48.1.51.43478

Zeng, Z., Ziegler, A.D. Searchinger, T., Yang, L., Chen, A., Ju, K., Piao, S., Li, L.Z., Ciais, P.,Chen, D., 2019. A reversal in global terrestrial stilling and its implications for wind energy production, Nature Climate Change 9, 979-985. https://www.nature.com/articles/s41558-019-0622-6

Zhang, J., Zhao, P., Wang, X., Zhang, J., Liu, J., Li, B., Zhou, Y., Wang, H., 2020. Main Factors Influencing Winter Visibility at the Xinjin Flight College of the Civil Aviation Flight University of China. Advances in Meteorology. 2020. https://doi.org/10.1155/2020/8899750

Zhang, W., Dong, X., Liu, Z., Lin, R., Luo, H., 2021. Influence of Decadal Ocean Signals on Meteorological Conditions Associated With the Winter Haze Over Eastern China. Frontiers in Environmental Science. 9, 727180. https://doi.org/10.3389/fenvs.2021.727180

Zhao, W., Chen, S., Zhang, H., Wang, J., Chen, W., Wu, R., Xing, W., Wang, Z., Hu, P., Piao, J., 2022. Distinct Impacts of ENSO on Haze Pollution in the Beijing–Tianjin–Hebei Region between Early and Late Winters. Journal of Climate. 35, 687-704. https://doi.org/10.1175/JCLI-D-21-0459.1

Zhao, S., Zhang, H., Xie, B., 2018. The effects of El Niño–Southern Oscillation on the winter haze pollution of China. Atmospheric Chemistry and Physics. 18, 1863-1877. https://doi.org/10.5194/acp-18-1863-2018

Zhao, Z., Liu, R., Zhang, Z., 2020. Characteristics of winter haze pollution in the Fenwei plain and the possible influence of EU during 1984–2017. Earth and Space Science. 7, e2020EA001134. https://doi.org/10.1029/2020EA001134

ArcGis 10.8, Desktop Help, 2021.

https://air.tehran.ir/(last accessed 15 October, 2022)

https://ccia.tehran.ir/ (last accessed 15 October, 2022)

https://cds.climate.copernicus.eu/cdsapp/dataset/reanalysis-era5-land (last accessed 27 November, 2022)

https://ier.tums.ac.ir/(last accessed 27 November, 2022)

http://tmy2.ir/ (last accessed 27 November, 2022)

Statistical Center of Iran, 2022, https://www.amar.org.ir.

www.irimo.ir (last accessed 27 November, 2022)